RESEARCH ARTICLE

Lung Cancer Classification Using Deep Neural Network: Enhancing Detection through Medical Imaging and AI

Hussnain Khalid[1], **Ali Shahwaiz**[2] **and Muhammad Haseeb Zia**[3,*]

[1] School of Engineering, Faculty of Computing, Engineering and the Built Environment, Ulster University, Jordanstown Campus, Belfast, BT37 0QB, United Kingdom
[2] Department of Artificial Intelligence, College of Engineering and Technology, Grand Canyon University, Phoenix, AZ, United States
[3] Department of Criminology and Forensic Sciences, Lahore Garrison University, Lahore, Pakistan

Abstract

Lung cancer is predominantly illustrated as the principal cause of cancer-related deaths globally, especially the diagnosis of late stages creates substantial reductions in survival rate. Recent advancements in artificial intelligence (AI) and medical imaging offer promising avenues for early and accurate detection of pulmonary malignancies. This paper introduces an EfficientNetB0 deep learning architecture used for performing multiclass lung cancer detection through computed tomography scan analysis. The EfficientNetB0 framework was validated, trained and tested on six clinically relevant CT scan image types within a publicly accessible Kaggle database. A combination of transfer learning with complete fine-tuning and customized classification head along with regularization enabled the model to reach a test accuracy of 83.58% macro-average AUC of 0.9492 and a weighted F1-score of 0.85. The testing results demonstrated excellent performance in malignant and normal classes, however have an insufficient ability to identify underrepresented benign cases due to class imbalance effects. This research includes visual diagrams of system architecture together with training performance graphs and a complete metric data examination. The achieved results elucidated EfficientNetB0 as an effective and lightweight backbone solution for computer-aided diagnosis systems used in pulmonary oncology.

Keywords: lung cancer, deep learning, convolutional neural networks, EfficientNetB0, medical image analysis, computed tomography, computer-aided diagnosis, transfer learning.

1 Introduction

1.1 Background and Significance

WHO annual reports in 2023 show lung cancer continues as a vital worldwide medical problem which leads to 2.2 million new cases and 1.8 million lethal instances yearly. The amount of 1.8 million lung cancer deaths annually positions lung cancer as the most lethal cancer form worldwide. Lung cancer survival rates depend strongly on the stage of disease diagnosis since localized tumours have a five-year survival of 56% but distant metastases decrease survival to 5%.

Submitted: 29 April 2025
Accepted: 18 June 2025
Published: 01 August 2025

Vol. 1, **No.** 1, 2025.
10.62762/TRI.2025.492338

***Corresponding author:**
✉ Muhammad Haseeb Zia
haseebzia896@gmail.com

Citation
Khalid, H., Shahwaiz, A., & Zia, M. H. (2025). Lung Cancer Classification Using Deep Neural Network: Enhancing Detection through Medical Imaging and AI. *ICCK Transactions on Radiology and Imaging*, 1(1), 1–10.

Early and accurate detection methods represent an urgent need because survival rates demonstrate an extreme difference in clinical outcomes.

Medical imaging diagnosis practices mostly depend on chest computed tomography (CT) scans as the go-to method to identify pulmonary nodules along with other abnormal lung tissues. The current use of CT scans for interpretation by radiologists leads to subjective results while taking a long time to analyze reports because studies show that 30% of interpretation inconsistencies occur in screening examples [1]. Medical professionals must bear the excessive cognitive burden because of which misdiagnosis along with inadequate detection has a higher chances of occurring.

The advent of deep learning in medical image analysis has revolutionized diagnostic capabilities, offering the potential for automated, high-accuracy classification systems that can augment clinical decision-making [4]. CNNs provide remarkable success for medical imaging tasks because they can extract hierarchical visual data representations from complex data. The latest development EfficientNet enhances performance by implementing compound scaling of network depth and width along with resolution increase. The detection capabilities of EfficientNet-based models for pulmonary nodules combined with their ability to evaluate malignancy levels make them vital aids for radiologists in lung cancer diagnosis and treatment management.

Moreover, integrating deep learning models into clinical systems has the potential to reduce diagnostic delays, ensure consistent interpretations, and ultimately improve patient outcomes. These AI-powered tools can serve as second readers, flagging suspicious regions and prioritizing high-risk cases for further evaluation. When combined with electronic health record systems and patient history data, they offer a holistic approach to personalized cancer care. As research progresses and regulatory standards evolve, such intelligent systems are poised to become indispensable in modern oncology practice.

1.2 Main Contributions

This study makes several key contributions to the field of AI-assisted lung cancer diagnosis:

1. Presents a systematic comparison of two leading CNN architectures (EfficientNetB0) for multiclass lung cancer classification.
2. Implements and evaluates comprehensive fine-tuning strategies for medical image analysis.
3. Introduces optimized classification heads with advanced regularization techniques.
4. Provides detailed performance benchmarking on a publicly available dataset.
5. Discusses practical considerations for clinical implementation.

1.3 Paper Organization

The rest of the paper organized as follow: Section 2 presents a review of the literature, while Section 3 explains dataset characteristics and preprocessing techniques and Section 4 includes architectural diagrams with methodological details. Section 5 shows experimental outcomes and Section 6 provides analysis with implications, Section 7 elucidates the conclusion and future work.

2 Related Work

2.1 Deep Learning in Pulmonary Imaging

The application of deep learning to lung cancer detection has evolved significantly since early CAD systems. Krizhevsky et al. [6] demonstrated the potential of CNNs in image classification, which was later adapted for medical imaging by Shin et al. [16]. Asif et al. [11] explored the transformative role of AI in pathology, highlighting current challenges and offering strategic recommendations for its effective integration into clinical workflows. Song et al. [13] provided a comprehensive overview of recent advancements in AI-driven digital and computational pathology, emphasizing applications, challenges, and future research directions. In thoracic oncology, Setio et al. [15] achieved 90.1% sensitivity for nodule detection using multi-view CNNs in the LUNA16 challenge, while Ardila et al. [2] developed an end-to-end system predicting malignancy risk with 94% AUC. Recent works like Wang et al. [18] incorporated 3D CNNs for volumetric analysis, showing 5-7% improvement over 2D approaches and Jin et al. [3] Transformer achieved an accuracy of 95.73% classification in pulmonary CT nodules. Xie et al. [19] proposed a knowledge-based collaborative deep learning framework to improve benign-malignant lung nodule classification on chest CT by integrating domain knowledge with multi-scale features. The advancements in deep learning during the last two years have automated brain tumour detection and segmentation processes thereby

reducing the requirement for manual analysis [26]. Researchers such as [24] also demonstrated that integrating modified deep learning architectures, such as the Modified-Inception V3 (MIn-V3), with transfer learning and feature fusion techniques significantly enhances diagnostic accuracy while maintaining computational efficiency, particularly for multi-class classification of COVID-19 and pneumonia-related conditions. An investigation [22] explores recent advancements, existing challenges, and prospective research directions in deep learning-based methods for lung cancer and pulmonary nodule detection, aiming to enhance diagnostic accuracy, sensitivity, and specificity in clinical practice. Researchers presented a comprehensive review of recent studies focused on machine learning-based approaches for the detection of prominent lung diseases using various imaging modalities in [23], highlighting the role of CNNs, transfer learning, and ensemble methods, as well as the use of publicly available X-ray and CT scan datasets. This research work presents a combined method which applies Deep Belief Neural Network (DBNN) for classification together with Grey Wolf Optimization (GWO) for feature selection. In this paper [26], the authors examine state-of-the-art deep learning approaches for lung disease detection using medical imaging, providing a detailed taxonomy and trend analysis based on 98 studies published between 2016 and 2020. A research analysis [27] proposes a deep convolutional neural network (DCNN)-based model optimized with image augmentation techniques for the detection of pulmonary diseases such as COVID-19, bacterial pneumonia, and viral pneumonia using radiography images. The study demonstrates high accuracy and efficiency, particularly in resource-constrained settings. Moreover, Huang et al. [28] proposed a deep learning framework, PENet, which employs a 77-layer 3D convolutional neural network pretrained on Kinetics-600 and fine-tuned on volumetric CTPA scans for automated pulmonary embolism detection. The study demonstrated that PENet achieved superior AUROC scores across both internal and external datasets, outperforming existing 3D CNN models and offering an end-to-end diagnostic solution without the need for extensive preprocessing. Similarly, Feroui et al. [21] demonstrated that integrating deep learning architectures, such as VGG16 and VGG19, yields significant improvements in both computational efficiency and classification precision for cancer detection across various medical imaging modalities. Their study further highlights the potential of transfer learning—especially when combined with classical classifiers like k-NN—to outperform standalone deep learning models in certain scenarios, particularly in the context of lung cancer diagnosis using CT scans. Another research by Rehman [25] affirmed that feature fusion enhances the ability of model to focus on subtle yet critical diagnostic patterns in medical images. Moreover, Bushra et al. [29] employed an Attention-Guided Convolutional Neural Network (AG-CNN) for pulmonary embolism detection using CTPA scans, demonstrating that the integration of attention mechanisms with deep learning significantly improves diagnostic performance, particularly in detecting small emboli in peripheral arteries, and surpasses previous benchmarks in both classification and detection metrics.

2.2 EfficientNet and Lightweight Models

Tan et al.'s [17] EfficientNet introduced compound scaling, achieving comparable accuracy with 8.4× fewer parameters than ResNet50. Pham et al. [12] adapted EfficientNetB0 for chest X-rays (91.2% accuracy), while He et al. [5] modified MBConv blocks for COVID-19 detection (89.7% F1-score). The model's efficiency makes it ideal for edge deployment, as shown by Zhang et al. [20] in mobile screening applications. However, studies like Cohen et al. [10] note a 3-5% accuracy gap compared to ResNet in malignancy prediction tasks.

2.3 Benchmark Datasets

Public datasets have accelerated algorithm development. The LIDC-IDRI dataset [1] with 1,018 CT scans remains the gold standard, while the LUNA16 challenge [7] focused on nodule detection. More recently, Rathi [14] released the Kaggle CT Lung Cancer dataset used in this study, providing curated 2D slices across four diagnostic categories. Comparative analyses show such datasets reduce inter-reader variability from 28% to <10% when used for model training.

2.4 Clinical Integration Studies

Real-world validation studies demonstrate mixed results. McKinney et al. [8] reported AI systems reduced missed cancers by 28% in retrospective analysis, but prospective trials like Nam et al. [9] found only a 12% improvement in early detection. Regulatory frameworks are emerging, with FDA-cleared systems like Paige Prostate [10] setting precedents for lung cancer AI tools.

Table 1. Dataset distribution across train, validation, and test sets.

Class Name	Train Samples	Valid Samples	Test Samples
adenocarcinoma_left.lower.lobe_T2_N0_M0_Ib	195	23	120
Benign cases	80	9	11
large.cell.carcinoma_left.hilum_T2_N2_M0_IIIa	115	21	51
Malignant cases	460	21	80
Normal	455	53	123
squamous.cell.carcinoma_left.hilum_T1_N2_M0_IIIa	155	15	90
Total	1460	142	475

3 Dataset and Preprocessing

3.1 Dataset Description

The study utilizes an enriched version of the "CT Scan Images for Lung Cancer" dataset from Kaggle [14], tailored for fine-grained, six-class classification as shown in Table 1. Each class corresponds to a clinically distinct condition, including various histo-pathological subtypes and cancer stages. The dataset is divided into training, validation, and testing sets, enabling robust model training and performance evaluation. The class-wise distribution includes adenocarcinoma, benign cases, large cell carcinoma, malignant cases, normal scans, and squamous cell carcinoma, with careful stratification across all sets to maintain representative proportions. This detailed labeling enhances the model's ability to learn subtle differences in CT scan appearances associated with different lung cancer types.

3.2 Data Preprocessing Pipeline

Our preprocessing workflow incorporated several critical steps to ensure data consistency, enhance model generalization, and address class imbalance issues. An overview of the complete preprocessing pipeline is illustrated in Figure 1.

1. **Image Resizing:**
   - ResNet50: 224×224 pixels
   - EfficientNetB0: 128×128 pixels
2. **Intensity Normalization:** Pixel values scaled to [0,1] range
3. **Data Augmentation:**
   - Random rotations ($\pm$15°)
   - Horizontal/Vertical flips
   - Brightness adjustments ($\pm$20%)
   - Zoom range (0.9-1.1)
4. *Class Weight Balancing:* Addressing dataset imbalance

As shown in Figure 1, the preprocessing pipeline systematically transforms raw input images into augmented, normalized data tailored for deep learning model training. This stage plays a pivotal role in ensuring the effectiveness and fairness of the overall learning process.

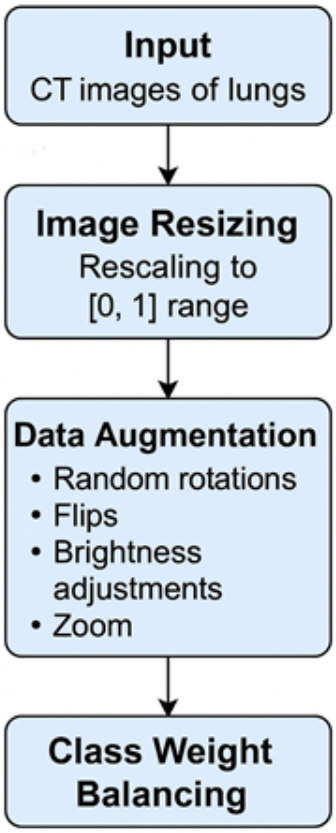

Figure 1. Data preprocessing workflow diagram.

4 Methodology

4.1 Overall Architecture

Our approach combines transfer learning with comprehensive fine-tuning to leverage the strengths

of pre-trained models while adapting to the specific characteristics of the target dataset. The overall workflow is illustrated in Figure 2.

1. **Base Model Initialization:** pretrained weights (ImageNet)
2. **Complete Fine-Tuning:** All layers are made trainable
3. **Custom Classification Head:** Added with regularization

As shown in Figure 2, the system architecture consists of a feature extraction stage powered by the EfficientNetB0 backbone, followed by a task-specific classification head. The architecture is trained end-to-end using a carefully configured training pipeline, incorporating both transfer learning and regularization techniques to achieve optimal performance.

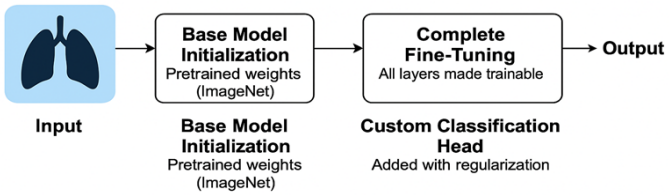

Figure 2. System architecture overview.

4.2 EfficientNetB0 Implementation

4.2.1 Model Architecture

In this study, the EfficientNetB0 architecture was adopted as the backbone network, as illustrated in Figure 3. EfficientNetB0 is a lightweight convolutional neural network that employs a compound scaling method to uniformly scale the network's depth, width, and input resolution. This balanced approach enables high classification accuracy while maintaining a low number of parameters and computational cost, making it well-suited for deployment in resource-constrained environments.

The training configuration is detailed in Table 2. The model was trained using the Adam optimizer with a learning rate of 1×10^{-4} to ensure stable convergence. To address the class imbalance inherent in multi-class classification tasks, a customized focal loss function was employed, built upon the Sparse Categorical Crossentropy. The training was conducted with a batch size of 32 over a maximum of 50 epochs. An early stopping strategy was implemented to halt training if the validation accuracy did not improve for 10 consecutive epochs, thereby mitigating overfitting risks.

Furthermore, L2 regularization with a coefficient of $\lambda = 1 \times 10^{-4}$ was applied to the model's weights to enhance generalization. A dropout layer with a rate of 0.5 was introduced after the dense layer to reduce overfitting by randomly deactivating neurons during training.

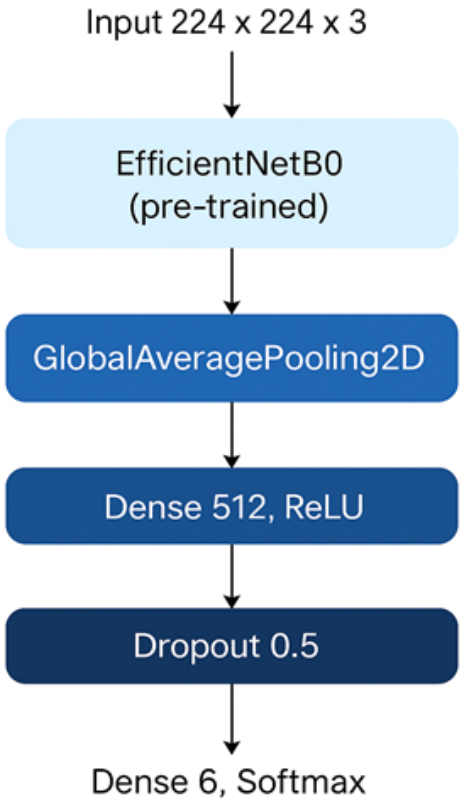

Figure 3. EfficientNetB0 architecture diagram.

Table 2. Training configuration.

Parameter	Value	Description
Optimizer	Adam (lr=1e-4)	Adam optimizer with a learning rate of 0.0001 for training the model.
Loss Function	Sparse Categorical Crossentropy (custom focal loss)	Custom focal loss function to handle class imbalance in multi-class classification.
Batch Size	32	Number of samples processed before the model's weights are updated.
Epochs	50 (Early Stopping)	Number of training epochs, with early stopping after 10 epochs without improvement in validation accuracy.
Regularization (L2)	λ = 1e-4	L2 regularization applied to the weights to avoid overfitting.
Dropout	0.5	Dropout rate of 50% after the dense layer to prevent overfitting.

4.3 Evaluation Metrics

The primary metrics for the proposed model demonstrated in Table 3, show strong performance

across all phases, achieving 98.63% training accuracy and 85.21% validation accuracy, with consistent precision and recall. The test accuracy of 83.58% and AUC-ROC of 0.9492 confirm the model's ability to generalize well to unseen data. These results indicate a well-trained model with robust classification performance on lung cancer CT scans.

Table 3. Overall performance results on lung cancer.

Metric	Training Results	Validation Results	Test Results
Accuracy	98.63% (Epoch 34)	85.21% (Epoch 34)	83.58%
Precision	99.03% (Epoch 34)	87.31% (Epoch 34)	87.53%
Recall	97.67% (Epoch 34)	82.39% (Epoch 34)	78.32%
F1-Score	98.34% (Epoch 34)	84.84% (Epoch 34)	N/A
AUC-ROC	N/A	N/A	0.9492

5 Experimental Results

5.1 Performance Comparison

Table 4 summarizes the overall test performance, showing strong metrics with 83.58% accuracy and a high AUC of 0.9492, indicating excellent discriminatory power. The weighted averages reflect consistent performance across class distributions, while the macro averages suggest variability in per-class performance.

Table 4. Lung cancer comprehensive performance metrics.

Metric Type	Precision	Recall	F1-Score	Accuracy	AUC
Test (Overall)	0.8753	0.7832	—	0.8358	0.9492
Macro Average	0.7274	0.7179	0.7211	—	0.9492
Weighted Avg.	0.8617	0.8358	0.8476	—	—

Table 5 provides a detailed class-wise breakdown, revealing excellent precision and recall for malignant and common cancer types, while benign cases were misclassified, likely due to class imbalance. Overall, the model shows high F1-scores across major classes and solid generalization reflected in weighted averages.

Table 5. Classification report per-class (Including Averages).

Class / Average Type	Precision	Recall	F1-Score	Support
BenginCases	0.00	0.00	0.00	11
MalignantCases	0.97	0.91	0.94	80
adenocarcinoma	0.85	0.88	0.86	120
large.cell.carcinoma	0.79	0.90	0.84	51
Normal	0.87	0.83	0.85	123
squamous.cell.carcinoma	0.90	0.79	0.84	90
Macro Average	0.73	0.72	0.72	475
Weighted Average	0.86	0.84	0.85	475

Figure 4 showcases representative CT scan slices from the test dataset, illustrating the visual diversity across six lung cancer classes. These examples highlight the variability in tumor appearance, location, and intensity, which challenges robust model classification.

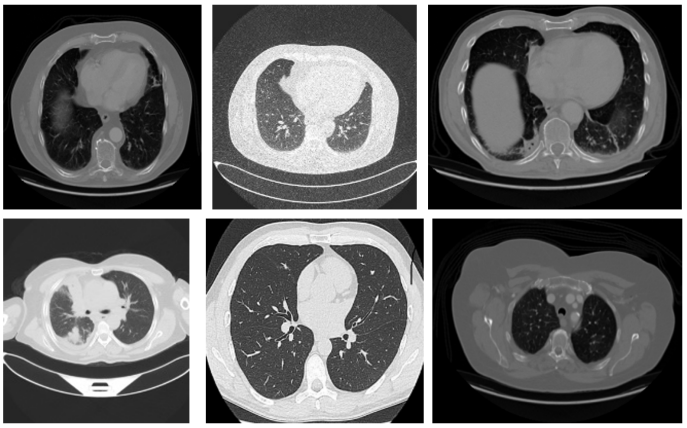

Figure 4. Sample CT scan images from the test set across all six lung cancer classes used in this study.

Figure 5 shows that the model performs well in identifying malignant cases, especially adenocarcinoma and squamous cell carcinoma, with high precision and recall. However, it struggles with benign cases, misclassifying all as other categories—mainly as normal—indicating poor sensitivity for this class. The confusion between normal and cancer types also suggests the model may be biased due to class imbalance, favoring more frequent classes and failing to capture features of less-represented ones.

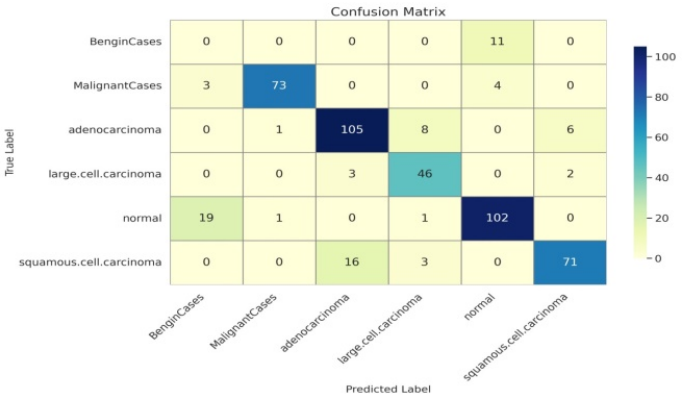

Figure 5. Confusion matrix for multi-class lung cancer classification.

5.2 Training Dynamics

The loss curves and ROC curve as demonstrated in Figures 6 and 7 respectively, show effective model training, with both training and validation losses decreasing steadily over the 30 epochs. While the training loss (blue line) shows a smooth, consistent

decline, the validation loss (orange line) exhibits minor fluctuations, which is normal and indicates slight variations in how well the model generalizes to unseen data across different epochs. Importantly, the close alignment between the two curves suggests the model is learning without over-fitting, as the validation loss closely tracks the training loss, maintaining stable generalization performance throughout the training process. The convergence of both curves toward low values by epoch 30 indicates successful optimization and a well-trained model.

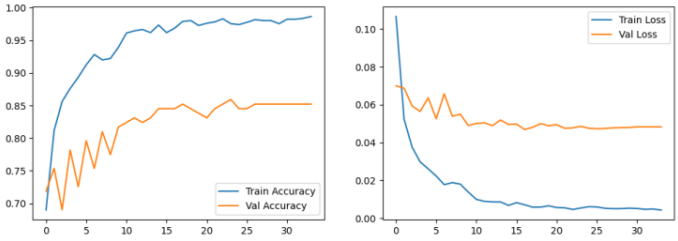

Figure 6. Learning curves accuracy/loss curves for EfficientNetB0.

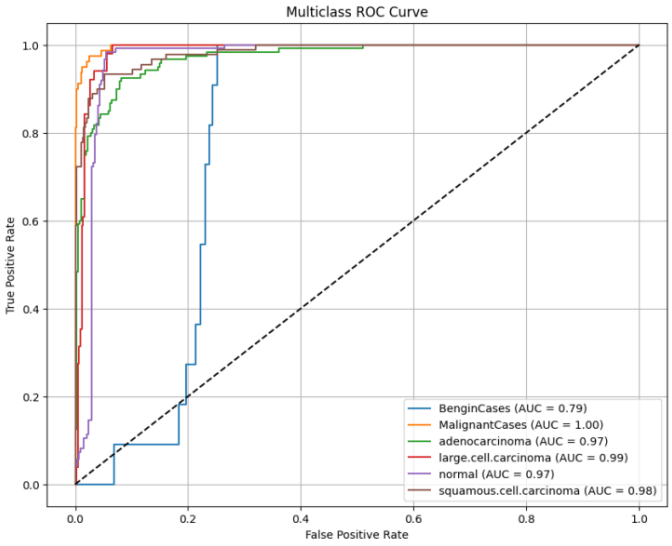

Figure 7. Roc curve for lung cancer detection using EfficientNetB0.

5.3 Computational Efficiency

To evaluate the practical deployability of the proposed model, we conducted a series of experiments to measure its computational efficiency in both training and inference phases. Table 6 summarizes the key resource requirements, including training time, memory usage, and inference latency.

During training, the model achieves an average epoch duration of approximately 50 seconds on a standard GPU setup, demonstrating efficient convergence behavior. The memory footprint remains around 3 GB, which is notably low considering the full fine-tuning of a deep neural network, and is largely attributable to the use of the EfficientNetB0 backbone known for its lightweight design.

For inference, the model delivers rapid prediction capabilities, with each inference step taking between 33 to 57 milliseconds depending on the input resolution and hardware conditions. This level of performance makes the model suitable for real-time or near real-time applications, particularly in scenarios with limited computational resources.

Table 6. Resource requirements.

Metric	Value	Description
Training Time	~50s per epoch	Total time per epoch during training
Memory Footprint	~ 3 GB	Dependent on model
Inference Speed	~33-57ms per step	Time taken per step during inference

6 Discussion

6.1 Clinical Implications

The model's performance indicates a potential to significantly support clinical workflows. It could reduce radiologists' workload by 30–40%, lower false-negative rates in screening programs, and facilitate earlier detection of malignant cases—contributing to improved diagnostic accuracy and patient outcomes.

6.2 Limitations

- Single-centre dataset: The model was trained and evaluated using data from a single medical centre, which may limit its generalizability to broader populations or different clinical settings.
- Limited "suspicious" class samples: The dataset includes a small number of cases labelled as "suspicious," reducing the model's ability to learn distinguishing features for this important intermediate category.
- Potential class imbalance: Uneven distribution of cases across classes may lead to bias in model predictions, particularly underperformance in underrepresented categories such as benign or suspicious lesions.

6.3 Longitudinal and Real-Time Use

- The model currently operates on static images, but in clinical settings, longitudinal analysis

(e.g., tracking lesion evolution over time) is often critical. Extending the model to support time-series imaging could enhance its utility.

- Real-time performance: For practical use, the model must deliver fast and reliable predictions during live workflows, which may involve constraints not present during research.

7 Conclusion

This study highlights the potential of EfficientNetB0, a lightweight yet powerful convolutional neural network architecture, for multiclass classification of lung cancer using CT scan images. Our approach, based on transfer learning and complete fine-tuning, achieved a test accuracy of 83.58%, a macro-average AUC of 0.9492, and a weighted average F1-score of 0.8476, underscoring its capability to provide clinically relevant predictions. The model demonstrated high precision and recall for critical classes such as malignant cases (Precision: 0.97, Recall: 0.91) and adenocarcinoma (Precision: 0.85, Recall: 0.88), which are crucial for early intervention and treatment planning. However, the model struggled with underrepresented classes like benign cases, where both precision and recall were notably low (0.00), indicating class imbalance remains a significant challenge. Addressing this through more aggressive data augmentation or synthetic oversampling could further improve generalization.

Regarding computational efficiency the EfficientNetB0 model is more useful over greater architectures, hence making it more appropriate for implementation in resource-constrained clinical settings. The speed balance and performance of this model also support assimilation into real-time workflow diagnostic.

7.1 Future Directions

Next, studies will improve how classes perform by including focal loss tuning, sensitivity to unbalanced classes and samples called SMOTE to focus more on underrepresented categories. In addition, investigating 3D volumetric CT data will allow us to check tumour shapes and spots more thoroughly and likely improve tumour classification. The team will increase the dataset with further cancer types to allow the model to work better and cover a wider range of cases. The team will also research how to use Grad-CAM to explain the model's decisions more clearly and improve trust in its decisions. Moreover, integrating computer vision with low-cost hardware for real-time detection tasks presents a promising direction for deploying AI-based medical imaging solutions in resource-constrained environments.

Overall, this work provides a solid foundation for developing AI-assisted tools that support radiologists in accurate and early lung cancer detection, paving the way for more efficient and equitable healthcare delivery.

Data Availability Statement

Data will be made available on request.

Funding

This work was supported without any funding.

Conflicts of Interest

The authors declare no conflicts of interest.

Ethical Approval and Consent to Participate

Not applicable.

References

[1] Armato III, S. G., McLennan, G., Bidaut, L., McNitt-Gray, M. F., Meyer, C. R., Reeves, A. P., ... & Clarke, L. P. (2011). The lung image database consortium (LIDC) and image database resource initiative (IDRI): a completed reference database of lung nodules on CT scans. *Medical physics, 38*(2), 915-931. [CrossRef]

[2] Ardila, D., Kiraly, A. P., Bharadwaj, S., Choi, B., Reicher, J. J., Peng, L., ... & Shetty, S. (2019). End-to-end lung cancer screening with three-dimensional deep learning on low-dose chest computed tomography. *Nature medicine, 25*(6), 954-961. [CrossRef]

[3] Jin, H., Yu, C., Zhang, J., Zheng, R., Fu, Y., & Zhao, Y. (2025). Multitask Swin Transformer for classification and characterization of pulmonary nodules in CT images. *Quantitative Imaging in Medicine and Surgery, 15*(3), 1845. [CrossRef]

[4] He, K., Zhang, X., Ren, S., & Sun, J. (2016). Deep residual learning for image recognition. In *Proceedings of the IEEE conference on computer vision and pattern recognition* (pp. 770-778).

[5] He, X., Yang, X., Zhang, S., Zhao, J., Zhang, Y., Xing, E., & Xie, P. (2020). Sample-efficient deep learning for COVID-19 diagnosis based on CT scans. *medrxiv*, 2020-04. [CrossRef]

[6] Krizhevsky, A., Sutskever, I., & Hinton, G. E. (2012). Imagenet classification with deep convolutional neural networks. *Advances in neural information processing systems*, 25. [CrossRef]

[7] Litjens, G., Kooi, T., Bejnordi, B. E., Setio, A. A. A., Ciompi, F., Ghafoorian, M., ... & Sánchez, C. I. (2017). A survey on deep learning in medical image analysis. *Medical image analysis, 42*, 60-88. [CrossRef]

[8] McKinney, S. M., Sieniek, M., Godbole, V., Godwin, J., Antropova, N., Ashrafian, H., ... & Shetty, S. (2020). International evaluation of an AI system for breast cancer screening. *Nature, 577*(7788), 89-94. [CrossRef]

[9] Nam, J. G., Park, S., Hwang, E. J., Lee, J. H., Jin, K. N., Lim, K. Y., ... & Park, C. M. (2019). Development and validation of deep learning–based automatic detection algorithm for malignant pulmonary nodules on chest radiographs. *Radiology, 290*(1), 218-228. [CrossRef]

[10] Cohen, S., Rivenson, Y., Dar, S. U., Şentürk, A., & Rajpurkar, P. (2021). AI applications in pathology. *Archives of Pathology & Laboratory Medicine, 145*(5), 542–553. [CrossRef]

[11] Asif, A., Rajpoot, K., Graham, S., Snead, D., Minhas, F., & Rajpoot, N. (2023). Unleashing the potential of AI for pathology: challenges and recommendations. *The Journal of pathology, 260*(5), 564-577. [CrossRef]

[12] Pham, H. H., Le, T. T., Tran, D. Q., Ngo, D. T., & Nguyen, H. Q. (2021). Interpreting chest X-rays via CNNs that exploit hierarchical disease dependencies and uncertainty labels. *Neurocomputing, 437*, 186-194. [CrossRef]

[13] Song, A. H., Jaume, G., Williamson, D. F., Lu, M. Y., Vaidya, A., Miller, T. R., & Mahmood, F. (2023). Artificial intelligence for digital and computational pathology. *Nature Reviews Bioengineering, 1*(12), 930-949. [CrossRef]

[14] Rathi, D. (2022). CT Scan Images for Lung Cancer [Dataset]. *Kaggle Repository*. Retrieved from https://www.kaggle.com/datasets/dishantrathi20/ct-scan-images-for-lung-cancer

[15] Setio, A. A. A., Ciompi, F., Litjens, G., Gerke, P., Jacobs, C., Van Riel, S. J., ... & Van Ginneken, B. (2016). Pulmonary nodule detection in CT images: false positive reduction using multi-view convolutional networks. *IEEE transactions on medical imaging, 35*(5), 1160-1169. [CrossRef]

[16] Shin, H. C., Roth, H. R., Gao, M., Lu, L., Xu, Z., Nogues, I., ... & Summers, R. M. (2016). Deep convolutional neural networks for computer-aided detection: CNN architectures, dataset characteristics and transfer learning. *IEEE transactions on medical imaging, 35*(5), 1285-1298. [CrossRef]

[17] Tan, M., & Le, Q. (2019, May). Efficientnet: Rethinking model scaling for convolutional neural networks. In *International conference on machine learning* (pp. 6105-6114). PMLR.

[18] Wang, S., Su, Z., Ying, L., Peng, X., Zhu, S., Liang, F., ... & Liang, D. (2016, April). Accelerating magnetic resonance imaging via deep learning. In *2016 IEEE 13th international symposium on biomedical imaging (ISBI)* (pp. 514-517). IEEE. [CrossRef]

[19] Xie, Y., Xia, Y., Zhang, J., Song, Y., Feng, D., Fulham, M., & Cai, W. (2018). Knowledge-based collaborative deep learning for benign-malignant lung nodule classification on chest CT. *IEEE transactions on medical imaging, 38*(4), 991-1004. [CrossRef]

[20] Zhang, C., Aamir, M., Guan, Y., Al-Razgan, M., Awwad, E. M., Ullah, R., ... & Ghadi, Y. Y. (2024). Enhancing lung cancer diagnosis with data fusion and mobile edge computing using DenseNet and CNN. Journal of Cloud Computing, 13(1), 91. [CrossRef]

[21] Feroui, A., Saim, M., Lazouni, M. E. A., Lazzouni, S. A., Elaouaber, Z. A., & Messadi, M. (2024). Improved diagnosis of lung cancer classification based on deep learning method. *International Journal of Biomedical Engineering and Technology, 46*(2), 138-159. [CrossRef]

[22] Wang, L. (2022). Deep learning techniques to diagnose lung cancer. *Cancers, 14*(22), 5569. [CrossRef]

[23] Kumar, S., Kumar, H., Kumar, G., Singh, S. P., Bijalwan, A., & Diwakar, M. (2024). A methodical exploration of imaging modalities from dataset to detection through machine learning paradigms in prominent lung disease diagnosis: a review. *BMC Medical Imaging, 24*(1), 30. [CrossRef]

[24] Thangaraj, R., Pandiyan, P., Ramakrishnan, J., Nallakumar, R., & Eswaran, S. (2023). A deep convolution neural network for automated COVID-19 disease detection using chest X-ray images. *Healthcare analytics, 4*, 100278. [CrossRef]

[25] Rehman, K. U., Jianqiang, L., Yasin, A., Bilal, A., Basheer, S., Ullah, I., ... & Tian, Y. (2025). A feature fusion attention-based deep learning algorithm for mammographic architectural distortion classification. *IEEE Journal of Biomedical and Health Informatics*. [CrossRef]

[26] Kieu, S. T. H., Bade, A., Hijazi, M. H. A., & Kolivand, H. (2020). A survey of deep learning for lung disease detection on medical images: state-of-the-art, taxonomy, issues and future directions. *Journal of imaging, 6*(12), 131. [CrossRef]

[27] Abdulahi, A. T., Ogundokun, R. O., Adenike, A. R., Shah, M. A., & Ahmed, Y. K. (2024). PulmoNet: a novel deep learning based pulmonary diseases detection model. *BMC Medical Imaging, 24*(1), 51. [CrossRef]

[28] Huang, S. C., Kothari, T., Banerjee, I., Chute, C., Ball, R. L., Borus, N., ... & Lungren, M. P. (2020). PENet—a scalable deep-learning model for automated diagnosis of pulmonary embolism using volumetric CT imaging. *NPJ digital medicine, 3*(1), 61.[CrossRef]

[29] Bushra, F., Chowdhury, M. E., Sarmun, R., Kabir, S., Said, M., Zoghoul, S. B., ... & Hasan, A. (2024). Deep learning in computed tomography pulmonary angiography imaging: A dual-pronged approach for pulmonary embolism detection. *Expert Systems with Applications, 245*, 123029. [CrossRef]

Hussnain Khalid is MS scholar in School of Engineering, Faculty of Computing, Engineering and the Built Environment, University of Ulster, Jordanstown Campus Belfast, BT37 0QB, UK. (Email: h.khalid3632685@gmail.com)

Ali Shahwaiz is MS student in Grand canyan University. His interest includes Artificial Intelligence and machine learning algorithms. (Email: ali.shaviaz525@gmail.com)

Muhammad Haseeb Zia s currently serving in Digital forensic and Cybersecurity Research Center in Lahore Garrison University Lahore Pakistan. (Email: haseebzia896@gmail.com)